

# The fission yeast chromo domain encoding gene *chp1*<sup>+</sup> is required for chromosome segregation and shows a genetic interaction with alpha-tubulin

Claudette L. Doe, Gouzheng Wang<sup>1</sup>, Cheok-man Chow, Mark D. Fricker<sup>2</sup>, Prim B. Singh<sup>1</sup> and E. Jane Mellor\*

Microbiology Unit, Department of Biochemistry, University of Oxford, South Parks Road, Oxford OX1 3QU, UK,

<sup>1</sup>Department of Development and Genetics, The Babraham Institute, Babraham Hall, Babraham, Cambridge CB2 4AT, UK and <sup>2</sup>Department of Plant Sciences, University of Oxford, South Parks Road, Oxford OX1 3RB, UK

Received May 14, 1998; Revised and Accepted July 24, 1998

## ABSTRACT

In eukaryotes, the segregation of chromosomes is co-ordinated by the centromere and must proceed accurately if aneuploidy and cell death are to be avoided. The fission yeast centromere is complex, containing highly repetitive regions of DNA showing the characteristics of heterochromatin. Two proteins, Swi6p and Clr4p, that are associated with the fission yeast centromere also contain a chromo (chromatin organisation modifier) domain and are required for centromere function. We have analysed a novel fission yeast gene encoding a putative chromo domain called *chp1*<sup>+</sup> (chromo domain protein in *Schizosaccharomyces pombe*). In the absence of Chp1p protein, cells are viable but show chromosome segregation defects such as lagging chromosomes on the spindle during anaphase and high rates of minichromosome loss, phenotypes which are also displayed by *swi6* and *clr4*. A fusion protein between green fluorescent protein (GFP) and Chp1p, like Swi6p, is localized to discrete sites within the nucleus. In contrast to Swi6p and Clr4p, Chp1p is not required to repress silent mating-type genes. We demonstrate a genetic interaction between *chp1*<sup>+</sup> and alpha-tubulin (*nda2*<sup>+</sup>) and between *swi6*<sup>+</sup> and beta-tubulin (*nda3*<sup>+</sup>). Chp1p and Swi6p proteins may be components of the kinetochore which captures and stabilizes the microtubules of the spindle.

## INTRODUCTION

Centromeres are highly specialised structures which direct the segregation of the chromosomes during karyokinesis. At the centromere, a protein–DNA complex called the kinetochore is proposed to interact with the microtubules and plays a central role in the alignment of chromosomes at metaphase, and their separation during anaphase. The kinetochore may also have other functions including a role in the cell cycle checkpoint which

monitors the attachment of chromosomes to the spindle and which elicits a delay prior to anaphase (1). Proper kinetochore function is vital as an inability to faithfully segregate the chromosomes has a dramatic effect on the viability of an organism.

The centromeric function seems to be retained in all eukaryotes, yet the structure of the centromere is not conserved. In the budding yeast *Saccharomyces cerevisiae*, the functional centromeric region consists of only 125 bp of DNA, comprised of three distinct elements, CDEI, CDEII and CDEIII (2). In the fission yeast *Schizosaccharomyces pombe*, there are three chromosomes of 5.7, 4.6 and 3.5 Mb, bearing centromeres which generally encompass 40–100 kb of DNA and which are far more complex than those of budding yeast. Each is composed of a central core of ~5 kb, flanked by large, inverted regions of DNA, made up of direct and inverted repeat elements known as K, L, B and J elements (3). This arrangement has much in common with the centromeres of mammalian cells which are also highly complex and contain large arrays of repetitive satellite DNA.

Studies have been carried out to try to determine the minimal sequence requirement for a functional *S.pombe* centromere. Two elements, the central core and the K repeat, seemed to be required for the formation of an active centromere and together can create a functional centromere on a minichromosome (4). In particular, a 2.1 kb region of the K repeat, known as the centromere enhancer, is needed for centromere function and for the formation of a specialized chromatin structure at the central core (5), which does not seem to be composed of a regularly spaced nucleosomal array (6,7). A recent study has reported that the enhancer element itself is not essential but can be substituted for by other sequences which are able to establish an active centromere (8). In addition, small deletions within the central core region can also be tolerated. Such findings indicate that there is functional redundancy at the fission yeast centromere.

Much less is known about the protein components of the *S.pombe* centromere. The Abp1p (ARS-binding protein), also known as Cbp1p (centromere binding protein), is thought to be a centromeric protein (9,10), and has been shown to bind

\*To whom correspondence should be addressed. Tel: +44 1865 275303; Fax: +44 1865 275297; Email: emellor@worf.molbiol.ox.ac.uk

specifically *in vitro* to sites within the centromere central core, as well as within the K repeat. A second protein, Cbh (CENP-B homologue), has also been shown to bind to the centromere K repeat and is essential for cell viability (11). Sequence comparisons have shown that there is significant homology between both these protein sequences and the human CENP-B protein. Another protein, called Mis6p, was found to be specifically localized at the centromere throughout the cell cycle and is essential for cell viability (12). This protein affects the chromatin structure at the central core and it has been proposed that it plays a role in the orientation of the centromeres.

The proteins Swi6p, Rik1p and Clr4p, which are thought to interact (13), also function at the centromere. They are not specific centromere factors, however, because they also act at the telomeres and the silent mating-type loci. These regions are thought to contain heterochromatin which represses gene expression (13–15). Fluorescence *in situ* hybridisation (FISH) has been used to demonstrate that Swi6p protein localizes at all three of these loci. Analysis of the *swi6*, *clr4* and *rik1* mutation strain phenotypes has shown that they are sensitive to anti-microtubule drugs, have a high rate of minichromosome loss and alleviate the repression of marker genes placed at centromeric, telomeric and silent mating-type positions (13–15).

Interestingly, both Swi6p and Clr4p proteins contain a motif known as a chromo domain (16,17). This ~50 amino acid motif is conserved in a large number of proteins (18–20) and was first identified in two *Drosophila* proteins, HP1 (heterochromatin

associated protein 1) and Pc (Polycomb) (21). HP1 is involved in the heterochromatin-induced repression of gene activity, whilst Pc is a transcriptional repressor of the homeotic genes. The demonstration that Pc protein and the murine HP1-like protein, M32, localize to many euchromatic sites has also suggested that the assembly of heterochromatin-like domains within euchromatin is a widespread mechanism for regulating gene expression (18,22,23).

In this paper, we report the analysis of a novel fission yeast chromo domain protein which has been identified on chromosome 1 as part of the *S.pombe* sequencing project. This predicted 960 amino acid protein contains a single, classical chromo domain near to the N-terminus and our studies reveal that the encoded gene, *chp1*<sup>+</sup>, is required for accurate chromosome segregation but is distinct from the Swi6p and Clr4p centromeric chromo domain proteins. Our evidence indicates that there is an interaction between Chp1p and alpha-tubulin and we suggest that Chp1p is a component of the kinetochore which plays a role in stabilizing microtubules.

## MATERIALS AND METHODS

### Strains and growth conditions

The *S.pombe* strains used in this study are listed in Table 1. Procedures and media used for the routine growth and maintenance of *S.pombe* were according to (24).

**Table 1.** Yeast strains

Strains used in this study:		References:
Sp 557	<i>ura4-D18, leu1-32, ade6-M210, h<sup>-</sup></i>	P. Nurse
Sp 556/557	<i>ura4-D18/ura4-D18, leu1-32/leu1-32, ade6-M216/ade6-M210, h<sup>+</sup>/h<sup>-</sup></i>	P. Nurse
Sp PG335	<i>clr1-5, ura4-D18, leu1-32, ade6-M216, his2, h<sup>90</sup></i>	(39)
Sp EG388	<i>rik1-304, ura4-D18, leu1-32, h<sup>90</sup></i>	(40)
Sp AL91	<i>swi6::ura4<sup>+</sup>, ura4-D18, ade6-M216, h<sup>90</sup></i>	(16)
Sp KE108	<i>clr4-S5, ura4-D18, ade6-M216, h<sup>90</sup></i>	(34)
Sp ED974	<i>nda3-km311, leu1-32, h<sup>+</sup></i>	(36)
Sp <i>nda2</i>	<i>nda2-km52, leu1-32, h<sup>-</sup></i>	(36)
Strains created during this study:		
Sp OX13	<i>ura4-D18, leu1-32, ade6-704, h<sup>90</sup></i>	
Sp OX25	<i>swi6::ura4<sup>+</sup>, ura4-D18, leu1-32, ade6-M216, h<sup>90</sup></i>	
Sp OX39	<i>clr4-S5, ura4-D18, leu1-32, ade6-M210, h<sup>90</sup></i>	
Sp OX109	<i>ura4-D18, leu1-32, ade6-704, h<sup>+</sup> / Ch10-CN2::sup3-5</i>	
Sp OX110	<i>chp1<sup>+</sup>/chp1::ura4<sup>+</sup>, ura4-D18/ura4-D18, leu1-32/leu1-32, ade6-M216/ade6-M210, h<sup>+</sup>/h<sup>-</sup></i>	
Sp OX113	<i>chp1::ura4<sup>+</sup>, ura4-D18, leu1-32, ade6-M210, h<sup>+</sup></i>	
Sp OX116	<i>chp1::ura4<sup>+</sup>, ura4-D18, leu1-32, ade6-M216, h<sup>90</sup></i>	
Sp OX121	<i>chp1::ura4<sup>+</sup>, ura4-D18, leu1-32, ade6-704, h<sup>-</sup> / Ch10-CN2::sup3-5</i>	
Sp OX127	<i>nda3-km311, ura4-D18, leu1-32, h<sup>+</sup></i>	
Sp OX129	<i>swi6::ura4<sup>+</sup>, nda3-km311, ura4-D18, leu1-32, h<sup>-</sup></i>	
Sp OX130	<i>chp1::ura4<sup>+</sup>, nda3-km311, ura4-D18, leu1-32, ade6-M210, h<sup>-</sup></i>	
Sp OX157	<i>nda2-km52, ura4-D18, leu1-32, ade6-M210, h<sup>-</sup></i>	
Sp OX159	<i>chp1::ura4<sup>+</sup>, nda2-km52, ura4-D18, leu1-32, ade6-M210, h<sup>-</sup></i>	

**chp1<sup>+</sup> constructs**

*chp1<sup>+</sup>* constructs were prepared either by subcloning fragments excised from the *S.pombe* DNA containing cosmid c18G6 (25) or by PCR from the same cosmid. A plasmid was created using the *chp1<sup>+</sup>* 2.882 kb open reading frame (ORF) only, which was isolated by PCR using the cosmid c18G6 (25) as a template and was fully sequenced. This was cloned into the high expression level pREP1 vector or low expression level pREP81 vector (26) under the control of the plasmid *nmt* promoter. A green fluorescent protein (GFP)–Chp1 fusion protein construct was made using the 714 bp GFP ORF prepared by PCR, using the TU#58 wildtype GFP-containing plasmid (27) as a template. This was cloned at the 5' end of the *chp1<sup>+</sup>* gene to give an in-frame N'-terminal GFP fusion with the *chp1<sup>+</sup>* gene in the vector pREP1.

Another two plasmids were made using either the 4.88 kb *Bam*HI–*Apa*I or the 3.77 kb *Nde*I–*Sac*I DNA fragments containing the *chp1<sup>+</sup>* gene (Fig. 1B). Each fragment was cloned into the vector pREP81 (26) but in the reverse orientation to the plasmid promoter. *Schizosaccharomyces pombe* strains containing these constructs were grown in the presence of thiamine, which strongly represses the plasmid promoter, so that expression would only arise from the *chp1<sup>+</sup>* promoter region contained in the genomic DNA insert.

**Minichromosome stability assay**

The stability of minichromosome Ch10-CN2 (28) in fission yeast strains was determined using the method of Kipling and Kearsey (29), as described by Allshire *et al.* (15). In outline, cells were cultured in minimal media lacking adenine to select for the minichromosome, and then the same number of cells were inoculated onto plates with and without adenine, in duplicate. At the same time, cells from the culture were inoculated into non-selective media and grown for at least 15 generations before plating out as before.

**Thiabendazole experiments**

Exponentially growing cell cultures were concentrated to a density of  $2 \times 10^7$  cells/ml, serially diluted by a factor of 10, ranging from  $2 \times 10^7$  to  $2 \times 10^4$ , and 5  $\mu$ l of each dilution spotted onto complete media or selective minimal media plates containing thiabendazole (TBZ). Plates were incubated at 30°C for 3–5 days.

**Immunofluorescence**

Cells were fixed with 3% p-formaldehyde as described by Hagan and Hyams (30) and immunolocalization of tubulin was carried out with mouse TAT-1 antibody (31), with anti-mouse TRITC conjugate (Sigma) and DAPI as a counter stain. Methanol fixing of cells was also used.

**Microscopy**

Cells were observed using an Olympus BX50F fluorescence microscope using a 100 $\times$  oil immersion lens and photographed on Fuji G400 film. In addition, the three-dimensional distribution of GFP–Chp1p fluorescence was imaged using a BioRad MRC 600 inverted confocal microscope attached to a Nikon Diaphot. Cells were embedded in 18% gelatin and 8–10 serial optical images were collected with a focus increment of 0.5  $\mu$ m using a 60 $\times$  1.4NA oil

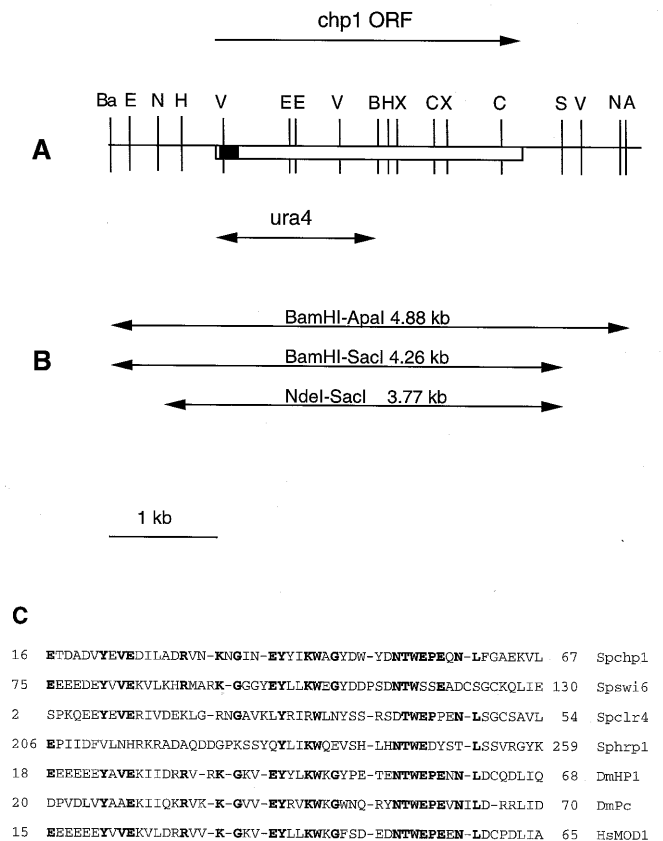


**Figure 1.** The *chp1<sup>+</sup>* gene. (A) Restriction map of the *chp1<sup>+</sup>* gene region. The open box and arrow indicate the 960 amino acid *chp1<sup>+</sup>* ORF and the black box represents the chromo domain. The region replaced by a 1.8 kb fragment containing the *ura4<sup>+</sup>* gene in the gene deletion experiment is indicated below the coding region. A, *Apa*I; B, *Bgl*III; Ba, *Bam*HI; C, *Clal*; E, *Eco*RI; H, *Hind*III; N, *Nde*I; S, *Sac*I; V, *Eco*RV; X, *Xho*I. (B) Fragments of *chp1<sup>+</sup>* used in complementation experiments. The arrows indicate the genomic fragments used in complementation experiments drawn in relation to the restriction map above. (C) Homology of the putative Chp1p chromo domain to other closely related chromo domain proteins. Alignment of the chromo domain motifs of Chp1p (Spchp1) with *S.pombe* Swi6p (Spswi6), Clr4p (Spclr4), and Hrp1p (Sphrp1), *Drosophila* HP1 and Pc (DmHP1 and DmPc, respectively) and human MOD1 (HsMOD1). Fission yeast Swi6p and human MOD1 are thought to be homologues of *Drosophila* HP1. Residues conserved in at least five out of the seven protein sequences are shown in bold. Numbers at each end represent amino acid residue numbers.

immersion lens, with excitation at 488 nm and viewed as a maximum projection.

**RESULTS****Sequence comparison**

The sequence of the *chp1<sup>+</sup>* gene was reported as part of the *S.pombe* chromosome I sequencing project (EMBL accession no. Z68198). The predicted ORF is of 960 amino acids, with no introns, giving a putative protein size of 108.7 kDa. This sequence predicts a chromo domain motif close to the N-terminus (Fig. 1). This motif is found also in the *S.pombe* *swi6<sup>+</sup>* (16), *clr4<sup>+</sup>* (17) and *hrp1<sup>+</sup>* (32) genes. A partial *S.pombe* sequence containing a chromo domain (33) has now been shown to be identical to the *clr4<sup>+</sup>* gene (17).

## Deletion of *chp1*<sup>+</sup>

To analyse the phenotype resulting from the absence of the Chp1p protein, a null allele was constructed. A plasmid was made in which the 1.5 kb fragment from the predicted start codon to the *Bgl*III site of the *chp1*<sup>+</sup> ORF was replaced with a 1.8 kb marker fragment containing the *ura4*<sup>+</sup> gene (Fig. 1). A linear 4.5 kb *Pst*I–*Sac*I fragment containing this deleted region was then used to transform a diploid, wildtype strain (Sp 556/557) to uracil prototrophy. Stable, diploid, *ura*<sup>+</sup> colonies were isolated (strain Sp OX110) and Southern analysis used to confirm that a copy of the *ura4*<sup>+</sup> gene had integrated at the *chp1*<sup>+</sup> locus (data not shown). The strains were sporulated and both tetrad and random spore analysis carried out. Haploid, *ura*<sup>+</sup> spores could be isolated showing that the Chp1p protein is not essential for cell viability. Two independent haploid isolates of the *chp1* deletion mutation strain were further checked by PCR analysis of genomic DNA using primers adjacent to the *chp1* deleted region and partial sequencing carried out (data not shown). This further verified that the *chp1*<sup>+</sup> gene had been deleted by a single copy of *ura4*<sup>+</sup> gene and that the ends of the integrated fragment had been resolved properly.

### *chp1*<sup>+</sup> does not affect switching ability at the mating-type locus

In fission yeast, a cell has either a plus or minus mating-type and this is determined by a copy of either plus or minus information present at the active mating-type locus. Silent, non-expressed copies of both genes are situated adjacent to the active locus, and can be copied into the active site allowing the cell to switch to the opposite mating-type. In *h*<sup>90</sup> strains, this switching occurs at high frequency leading to ~90% of cells being able to mate and sporulate.

In *swi6* and *clr4* mutation strains, the switching frequency is greatly reduced (16,34). It was therefore of interest to test the ability of the *chp1* deletion mutation strain to undergo switching. Several independent *h*<sup>90</sup> isolates of the *chp1* deletion mutation strain were induced to sporulate on low nitrogen media and were treated with iodine vapour which stains the starch in the spores. This revealed that the *chp1* mutation strain (Sp OX116) has a level of switching at the mating-type locus comparable to that of wildtype *h*<sup>90</sup> cells (Sp OX13) (Fig. 2).

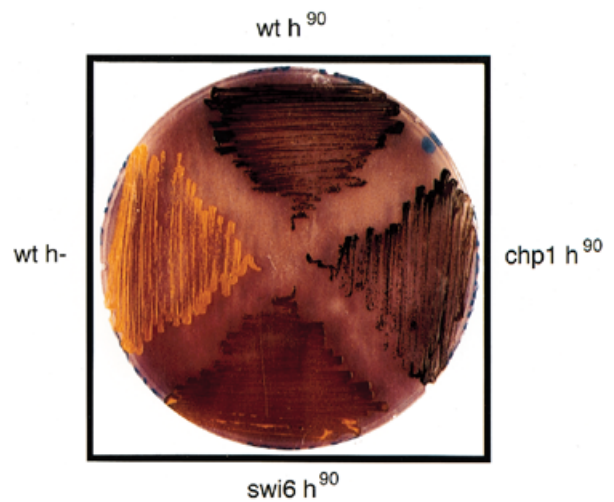


**Figure 2.** Mating-type switching ability of the *chp1* deletion mutation strain. A *chp1* deletion mutation *h*<sup>90</sup> strain (Sp OX116), a wildtype *h*<sup>90</sup> strain (Sp OX13), a *swi6* deletion mutation *h*<sup>90</sup> strain (Sp OX25) and a wildtype *h*<sup>-</sup> (non-switching) strain (Sp 557) were sporulated on low nitrogen media and stained with iodine vapour to show the starch containing spores (black).

### Increased rates of minichromosome loss in the *chp1* mutation strain

An investigation was carried out to determine whether Chp1p protein is required for chromosome segregation. The *chp1* mutation strain was assayed for defects in the transmission of chromosomes, using a *chp1* deletion mutation strain containing the Ch10-CN2 minichromosome. The Ch10-CN2 minichromosome is a linear, 120 kb derivative of chromosome III, containing a suppressor of the *ade6-704* mutation (28). The rate of loss of the minichromosome in the *chp1* deletion mutation strain was assayed by the ability of colonies to grow on media lacking adenine and compared to loss rate in the wildtype background. In the *chp1* mutation strain (Sp OX121), the minichromosome loss rate was significantly higher than in wildtype cells, with loss occurring in ~2.2% of divisions compared to no detectable loss in the wildtype strain (Sp OX109) (Table 2).

**Table 2.** The effect of the *chp1* mutation on the segregation of a minichromosome

Strain	T*	% Minichromosome loss per generation	<i>n</i> <sup>abc**</sup>
wt (Sp OX109)	–	0.0	3abc
<i>chp1::ura4</i> <sup>+</sup> (Sp OX121)	–	2.2	6aaaabb
<i>chp1::ura4</i> <sup>+</sup> (Sp OX121) + pREP1	+	2.3	9aaaaaaaa
<i>chp1::ura4</i> <sup>+</sup> (Sp OX121) + <i>Bam</i> HI– <i>Apa</i> I 4.88 kb	+	0.16	6aabbbb
<i>chp1::ura4</i> <sup>+</sup> (Sp OX121) + <i>Nde</i> I– <i>Sac</i> I 3.77 kb	+	0.38	4aaab
<i>chp1::ura4</i> <sup>+</sup> (Sp OX121) + pREP81– <i>chp1</i> <sup>+</sup>	–	0.43	4aaaa
<i>chp1::ura4</i> <sup>+</sup> (Sp OX121) + pREP1–GFP– <i>chp1</i> <sup>+</sup>	+	0.52	4aabc
<i>chp1::ura4</i> <sup>+</sup> (Sp OX121) + pREP1–GFP– <i>chp1</i> <sup>+</sup>	–	0.45	2aa

\*Presence or absence of 4 μM thiamine.

\*\*The number of independent experiments carried out, where abc is the approximate number of colonies per plate examined in each experiment, a = 100–500, b = 500–1000 and c = 1000–1500.

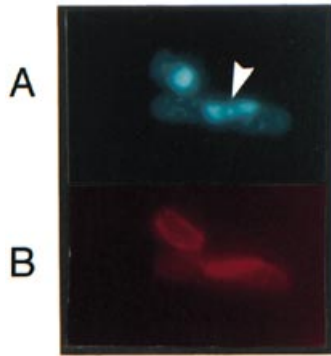


**Figure 3.** Aberrant chromosome segregation in *chp1* deletion mutation strain cells. An example of a fixed and immunofluorescent stained *chp1* deletion mutation cell (strain Sp OX113) is shown displaying a lagging chromosome during anaphase, (A) stained with DAPI and (B) stained with anti-tubulin antibody. The white arrowhead in (A) identifies the lagging chromosome. Cells were grown in complete media.

The ability of a number of *chp1*<sup>+</sup> genes containing plasmids to rescue the minichromosome loss phenotype was then tested. A construct containing just the *chp1*<sup>+</sup> ORF in the low expression level pREP81 expressed under non-repressing conditions was able to suppress the mutation strain phenotype. Plasmids containing a 4.88 kb *Bam*HI–*Apa*I or a 3.77 kb *Nde*I–*Sac*I genomic fragment (Fig. 1) cloned into pREP81 (26) but expressed from the *chp1*<sup>+</sup> promoter, were also able to restore the minichromosome loss rate to approaching wildtype levels (Table 2). An N-terminal tagged GFP–Chp1p in the high expression level pREP1 (26), expressed in both the presence or absence of repressing thiamine, showed complementation of the mutation phenotype. Cells transformed with the empty pREP1 vector alone did not show complementation of the phenotype.

#### *chp1* is associated with chromosome segregation defects

*chp1* null allele (Sp OX113) cells were visually analysed for chromosome segregation defects using indirect immunofluorescence with anti-tubulin (TAT-1) antibodies (31) and DAPI (4',6-diamidino-2-phenylindole) staining of the DNA. This analysis revealed that 7.8% (23/296) of late anaphase cells contained a lagging chromosome, whilst no lagging chromosomes could be detected in wildtype (Sp 557) cells. The spindles themselves appeared normal (Fig. 3).

#### Chp1 protein localizes to the nucleus

To determine the intracellular localization of the *chp1*<sup>+</sup> gene product, a construct was made containing the GFP (27) fused in-frame to the N-terminus of the *chp1*<sup>+</sup> gene. This fusion protein was able to rescue the *chp1* mutation phenotype in a similar manner to vectors expressing the untagged protein, suggesting a functional protein is produced. This construct was transformed into wildtype (Sp 557) cells which were grown in selective media in the absence of thiamine and were observed by UV or confocal microscopy. The GFP–Chp1 protein was found to localize within the nucleus as distinct spots (Fig. 4). Analysis of maximum projection confocal microscope images from 117 live, GFP-expressing cells indicated that in the majority (74%) of nuclei,

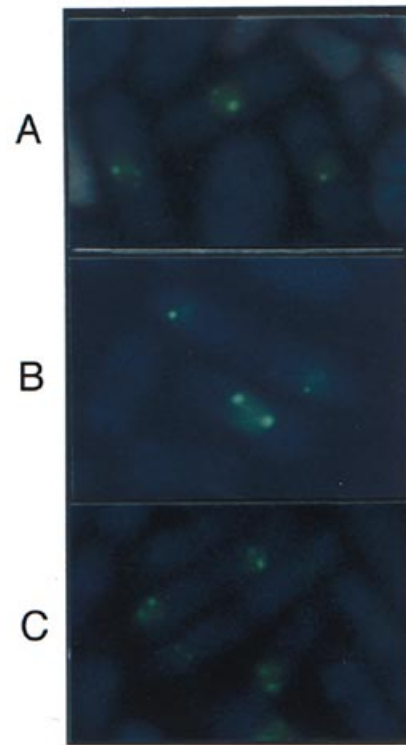


**Figure 4.** Localization of GFP–Chp1 protein. The live cell localization of the GFP–Chp1 protein in different strain backgrounds is shown; (A) wildtype (Sp 557), (B) *rik1* mutation strain (Sp EG388) and (C) *clr4* mutation strain (Sp OX39). Cells were grown in selective minimal media lacking leucine and in the absence of thiamine.

there were one or two spots; however, nuclei with three to five spots were also seen.

The fission yeast Swi6p protein also localizes as a few discrete spots within the nucleus; however, these become delocalized in the *clr4* and *rik1* mutation backgrounds (13). Studies of a plasmid expressed GFP–Swi6 fusion protein gives the same results (C.Chow, unpublished data). To investigate whether the Chp1p protein displays similar properties, we transformed the GFP–Chp1 fusion construct into *clr4* (Sp OX39) and *rik1* (Sp EG388) mutation backgrounds. In these strains the punctate nuclear localization is retained (Fig. 2). This distribution is also seen in *swi6* (Sp OX25), *chp1* (Sp OX113) and *clr1* (Sp PG335) mutation strain backgrounds (data not shown).

#### Sensitivity to anti-microtubule drugs is affected by *chp1*

The defective chromosome segregation observed in the *chp1* deletion mutation strain might be due to a defective interaction between the kinetochore and the spindle microtubules. To further elucidate this, the *chp1* mutation strain (Sp OX113) was tested for the ability to grow in the presence of the anti-microtubule drug, TBZ. The *chp1* mutation strain grew less well than wildtype (Sp 557) at both 10 and 20 µg/ml TBZ (Fig. 5).

The ability of *chp1*<sup>+</sup> gene containing plasmids to complement this TBZ sensitivity of the *chp1* mutation strain (Sp OX113) was then tested. A plasmid containing the 3.77 kb *Nde*I–*Sac*I genomic fragment (under the *chp1*<sup>+</sup> promoter) (Fig. 1) not only rescued the

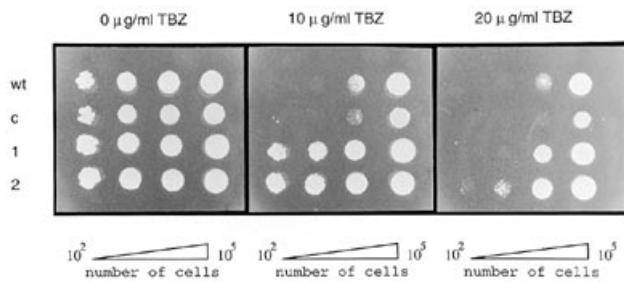


**Figure 5.** Sensitivity of *chp1* mutation strains to TBZ. Exponentially growing cells were serially diluted by 1/10 and spotted to selective minimal media lacking leucine and containing thiamine plus 0, 10 or 20  $\mu\text{g/ml}$  TBZ. Plates were grown at 30°C for 3 days. The strains are wildtype (Sp 557) carrying pREP1 empty vector (wt) and *chp1* deletion mutation cells (Sp OX113) carrying pREP1(c), *NdeI-SacI* 3.77 kb-pREP81 (1) and GFP-Chp1-pREP1 (2). The numbered triangles underneath the figure indicate the increasing number of cells spotted on the plate, going from  $1 \times 10^2$  to  $1 \times 10^5$  cells per spot from left to right.

TBZ sensitivity but also conferred increased resistance to TBZ compared to wildtype cells at both 10 and 20  $\mu\text{g/ml}$  TBZ (Fig. 5). A plasmid containing the larger 4.88 kb *BamHI-ApaI* genomic fragment (Fig. 1) behaved similarly (data not shown). Moreover, plasmids containing the *chp1*<sup>+</sup> ORF fused to GFP in pREP1 (Fig. 5) or the *chp1*<sup>+</sup> ORF alone in pREP1 (data not shown) also rescued the TBZ sensitivity of the *chp1* mutation strain and again resulted in increased TBZ resistance compared with wildtype cells. The effect is even more marked than that seen with the *NdeI-SacI* plasmid. The use of these different constructs appears to rule out the presence of mutations in the plasmid insert which might result in such resistance to TBZ. These observations were repeated using two independent isolates of the *chp1* deletion mutation strain. Both of these strains had been thoroughly checked, by Southern blotting, PCR and sequencing, to rule out the presence of additional mutations which might account for the TBZ resistance in *chp1*<sup>+</sup> plasmid containing strains.

To further investigate this finding, a linear *BamHI-SacI* 4.26 kb *chp1*<sup>+</sup> containing genomic DNA fragment (Fig. 1) was transformed into one of the *chp1::ura4*<sup>+</sup> deletion strains (Sp OX113). Transformants were selected on 5-fluoro-orotic acid (FOA) containing media on which only cells containing a defective or deleted *ura4*<sup>+</sup> gene can grow (35). This should select for cells where the *ura4*<sup>+</sup> containing disrupted copy of the *chp1*<sup>+</sup> gene has been replaced by the wildtype *chp1*<sup>+</sup> gene copy from the linear fragment. Southern blotting was used to confirm that a wildtype copy of *chp1*<sup>+</sup> had integrated at the *chp1::ura4*<sup>+</sup> site and growth on FOA was due to this, not due to mutation of the *ura4*<sup>+</sup> gene (data not shown). The growth on TBZ containing media of a correctly integrated isolate and a second incorrect isolate, which did not contain the *chp1*<sup>+</sup> gene and probably had a mutation in *ura4*<sup>+</sup>, was tested alongside a wildtype strain and the parental *chp1* mutation strain (Fig. 6). The correct strain, with an integrated copy of *chp1*<sup>+</sup>, showed the same pattern of TBZ sensitivity as the wildtype strain and did not show increased TBZ resistance like plasmid expressed *chp1*<sup>+</sup> strains did. The incorrect isolate behaved as the parent *chp1* deletion mutation strain did. Taken together, these results suggest that both the presence or absence of the Chp1p protein affects the stability of microtubules in the presence of TBZ.

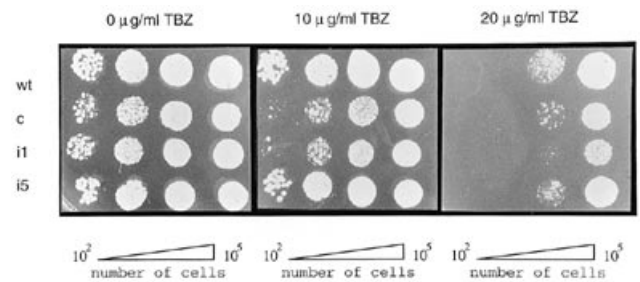


**Figure 6.** Sensitivity of *chp1*<sup>+</sup> integrant strains to TBZ. Exponentially growing cells were serially diluted by 1/10 and spotted to complete media containing 0, 10 or 20  $\mu\text{g/ml}$  TBZ. Plates were grown at 30°C for 3 days. The strains are (wt) wildtype (Sp 557), (c) *chp1* deletion mutation strain (Sp OX113), (i1) an incorrect *chp1* deletion mutation FOA isolate which does not contain the *chp1*<sup>+</sup> gene, and (i5) a *chp1* deletion mutation FOA isolate containing the correctly integrated *BamHI-SacI* 4.26 kb *chp1*<sup>+</sup> fragment at the *chp1::ura4*<sup>+</sup> locus. The numbered triangles underneath the figure indicate the increasing number of cells spotted on the plate, going from  $1 \times 10^2$  to  $1 \times 10^5$  cells per spot from left to right.

### *chp1* TBZ sensitivity compared with other strains

The sensitivity of the *chp1* deletion mutation strain (Sp OX113) to TBZ is greater than that of wildtype (Sp 557) but less than that of a *swi6* deletion mutation strain (Sp OX25) (Fig. 7). An *nda3* (beta-tubulin) mutation strain (Sp OX127) is more resistant to TBZ than both *chp1* and wildtype (Fig. 7) (36,37), whilst an *nda2* (alpha-tubulin) mutation strain (Sp OX157) is much more sensitive to TBZ than any of these strains (Fig. 8) (36,37).

### Interaction with tubulin

One explanation for the TBZ data is that the Chp1p protein might interact with microtubules, although the spindle immunofluorescence and localization data suggests that Chp1p is not likely to be a component of the spindle itself. Evidence for an interaction between Swi6p and beta-tubulin has been reported, where a *swi6 nda3* double mutation strain is supersensitive to cold, and has very high minichromosome loss rates (13). To investigate whether Chp1p acts in a similar manner, a double mutation of the *chp1* deletion mutation in combination with a cold sensitive beta-tubulin mutation, *nda3* (36), was created. This double mutation strain (Sp OX130) did not show any increased sensitivity to 10 or 20  $\mu\text{g/ml}$  TBZ at the *nda3* permissive temperature of 30°C compared with the *chp1* mutation strain (Sp OX113), which is the most TBZ sensitive of the single mutation strains (Fig. 7). The data thus gives no suggestion of an interaction between Chp1p protein and beta-tubulin. In contrast to this, in the same assay, a *swi6 nda3* double mutation strain (Sp OX129) was shown to be supersensitive to TBZ compared to both the *swi6* (Sp OX25) and *nda3* (Sp OX127) single mutation strains (Fig. 7).

The possibility of an interaction between Chp1p protein and alpha-tubulin was then tested using a double mutation strain of the *chp1* deletion mutation in combination with the cold sensitive alpha1-tubulin mutation, *nda2* (36,37). The *nda2* single mutation strain is very sensitive to TBZ so the sensitivity of the *chp1 nda2* double mutation strain was tested at TBZ concentrations of 0.5 and 1  $\mu\text{g/ml}$ . Our data show that at the *nda2* permissive temperature of 30°C, the *chp1 nda2* double mutation strain

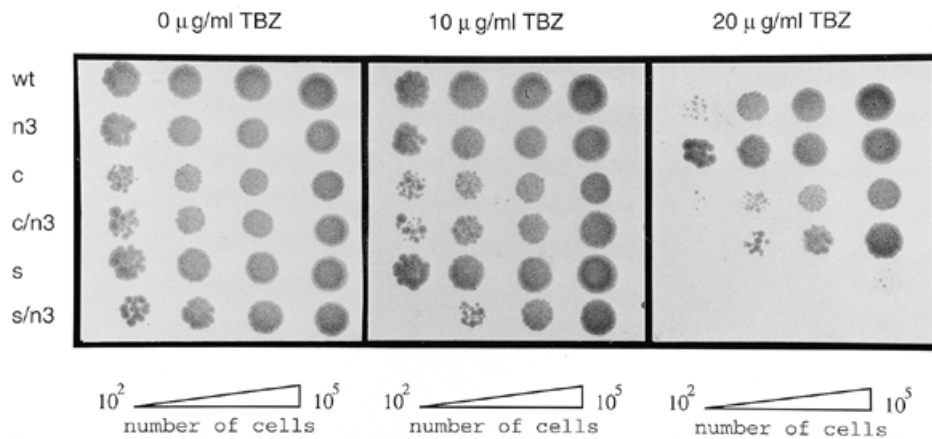


**Figure 7.** Sensitivity of *nda3* and *chp1* mutation strains to TBZ. Exponentially growing cells were serially diluted by 1/10 and spotted to complete media containing 0, 10 or 20 µg/ml TBZ. Plates were grown at 30°C for 3 days. The strains are (wt) wildtype (Sp 557), (n3) *nda3* (Sp OX127), (c) *chp1* (Sp OX113), (c/n3) *chp1 nda3* double mutation (Sp OX130), (s) *swi6* (Sp OX25) and (s/n3) *swi6 nda3* double mutation strain (Sp OX129). The numbered triangles underneath the figure indicate the increasing number of cells spotted on the plate, going from  $1 \times 10^2$  to  $1 \times 10^5$  cells per spot from left to right.

(Sp OX159) is much more sensitive to TBZ than a strain carrying either the *chp1* (Sp OX113) or *nda2* mutation (Sp OX157) alone. Significantly, the double mutation strain grown at 25°C also shows enhanced cold sensitivity (Fig. 8). This indicates that there is a genetic interaction between *chp1* and *nda2* mutations.

## DISCUSSION

The *chp1*<sup>+</sup> gene is the third distinct chromo domain encoding gene with a role in the segregation of fission yeast chromosomes. Another fission yeast chromo domain encoding gene, *hnp1*<sup>+</sup>, has also been reported, but it has not been analysed in respect of centromere defects. This gene is the *S.pombe* homologue of mouse CHD-1, and encodes putative chromo and helicase domains (32).

*chp1*<sup>+</sup> encodes a large protein (960 amino acids) of which the chromo domain represents only a small region (50 amino acids) at the N-terminus. In contrast, the Swi6p centromeric chromo domain containing protein is much smaller (the gene encodes 328 amino acids) and contains an N-terminal chromo domain, a hinge region and a C-terminal shadow chromo domain (19,20). These proteins may share the presence of a chromo domain but, not surprisingly, their functions appear to be distinct. *clr4* and *swi6* strains do share similar phenotypes and it is known that Clr4p, along with Rik1p, is required for the correct sub-nuclear localization of Swi6p to three distinct locations within the nucleus: the centromeres, telomeres and the mating-type loci (13). The discrete sub-nuclear distribution of Chp1p, however, is not affected by mutations in either *clr4*<sup>+</sup>, *rik1*<sup>+</sup> or *swi6*<sup>+</sup>. The majority of cells contain one or two distinct spots of Chp1p which, because of the nature of the Chp1p protein and the phenotypes associated with the gene deletion, would be consistent with an association with the centromeres and perhaps a second region, possibly the telomeres, which can also affect chromosome stability (38). It is not yet known whether Chp1p is actually localized at either of these sites and further experimentation will be needed to clarify this. We found no evidence of a role for Chp1p in repressing the silent mating-type loci. This suggests that

chromo domain proteins have discrete localization patterns and that the Chp1p protein has a distinct set of functions.

Nevertheless, the *chp1* strain has many similar phenotypes to those seen in *swi6* and *clr4* strains and these are consistent with a role for Chp1p at the centromere. *chp1* strains, like *swi6* and *clr4* strains, have a particular problem in the accurate segregation of chromosomes. The *chp1* strain is also sensitive to the anti-microtubule drug TBZ, as are *clr4* and *swi6* (14). This could be explained by a defect in the spindle checkpoint (1) allowing cells to divide in the absence of proper spindle formation. Alternatively, in these strains the microtubules themselves might be less stable or more sensitive to anti-microtubule drugs. In support of this second explanation, we found that increasing the *chp1*<sup>+</sup> copy number resulted in increased resistance to TBZ, perhaps reflecting an increased stability of the microtubules. The TBZ sensitivity in the absence of Chp1p might be explained by an inability of some of the kinetochores to effectively capture and stabilize the microtubules.

The link between chromo domain proteins and microtubules is further supported by genetic evidence. We have shown a genetic interaction between *swi6*<sup>+</sup> and *nda3*<sup>+</sup> (beta-tubulin) based on TBZ sensitivity. No such interaction could be shown between Chp1p and beta-tubulin; however, a genetic interaction could be established between *chp1*<sup>+</sup> and alpha-tubulin (*nda2*<sup>+</sup>) on the basis of cold sensitivity and TBZ sensitivity, although whether this is a direct or indirect interaction is not known.

The Chp1p chromo domain protein clearly has a role which is distinct from that of the other chromo domain proteins which act at the centromere. Chp1p and Swi6p both interact with tubulin, but apparently not through the same component. It will be interesting to investigate the Chp1p-tubulin interaction further, to see whether Chp1p does represent a kinetochore structural subunit or whether in fact it has an additional or different role such as the regulation of microtubule formation.

## ACKNOWLEDGEMENTS

We would like to thank the following people for the generous donation of strains, plasmids and antibodies: Paul Nurse,

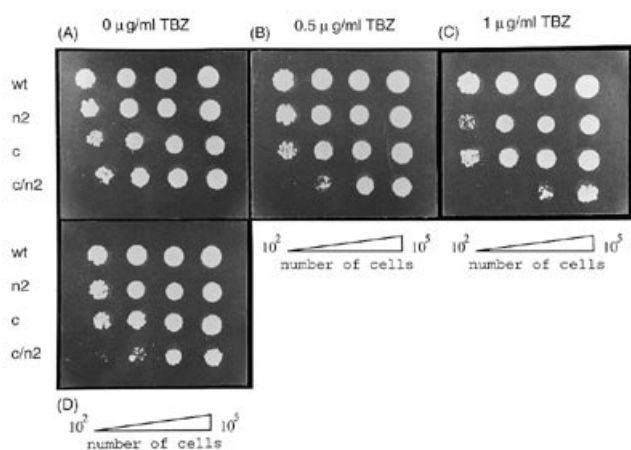


**Figure 8.** Sensitivity of *nda2* and *chp1* mutation strains to cold and the drug TBZ. Exponentially growing cells were serially diluted by 1/10 and spotted to complete media containing (A and D) 0, (B) 0.5 or (C) 1 µg/ml TBZ. Plates were grown at 30°C for 3 days (A–C) or 25°C for 5 days (D). The strains are (wt) wildtype (Sp 557), (n2) *nda2* (Sp OX157), (c) *chp1* (Sp OX113) and (c/n2) *chp1 nda2* double mutation strain (Sp OX159). The numbered triangles underneath the figure indicate the increasing number of cells spotted on the plate, going from  $1 \times 10^2$  to  $1 \times 10^5$  cells per spot from left to right.

Henning Schmidt, Peter Fantes, Richard Egel, Karl Ekwall, Amar Klar, Mitsuhiro Yanagida, Martin Chalfie, Bart Barrell and Keith Gull. We also thank Alex Morgan for photographic work. This work was supported by grants from the Wellcome Trust (C.L.D. and E.J.M.) and from the BBSRC (grant no. A01809) (G.W., C.C., M.D.F., P.B.S. and E.J.M.).

## REFERENCES

- Hardwick, K.G. (1998) *Trends Genet.*, **14**, 1–4.
- Pluta, A.F., Makay, A.M., Ainsztein, A.M., Goldberg, I.G. and Earnshaw, W.C. (1995) *Science*, **270**, 1591–1595.
- Steiner, N.C., Hahnenberger, K.M. and Clarke, L. (1993) *Mol. Cell. Biol.*, **13**, 4578–4587.
- Baum, M., Ngan, V.K. and Clarke, L. (1994) *Mol. Cell. Biol.*, **5**, 747–761.
- Marschall, L.G. and Clarke, L. (1995) *J. Cell. Biol.*, **128**, 445–454.
- Polizzi, C. and Clarke, L. (1991) *J. Cell. Biol.*, **112**, 191–201.
- Takahashi, K., Murakami, S., Chikashige, Y., Funabiki, H., Niwa, O. and Yanagida, M. (1992) *Mol. Biol. Cell*, **3**, 819–835.
- Ngan, V. and Clarke, L. (1997) *Mol. Cell. Biol.*, **17**, 3305–3314.
- Murakami, Y., Huberman, J.A. and Hurwitz, J. (1996) *Proc. Natl Acad. Sci. USA*, **93**, 502–507.
- Halverson, D., Baum, M., Stryker, J., Carbon, J. and Clarke, L. (1997) *J. Cell. Biol.*, **136**, 487–500.
- Lee, J., Huberman, J.A. and Hurwitz, J. (1997) *Proc. Natl Acad. Sci. USA*, **94**, 8427–8432.
- Saitoh, S., Takahashi, K. and Yanagida, M. (1996) *Cell*, **90**, 131–143.
- Ekwall, K., Nimmo, E.R., Javerzat, J., Borgstrom, B., Egel, R., Cranston, G. and Allshire, R. (1996) *J. Cell Sci.*, **109**, 2637–2648.
- Ekwall, K., Javerzat, J., Lorentz, A., Schmidt, H., Cranston, G. and Allshire, R. (1995) *Science*, **269**, 1429–1431.
- Allshire, R.C., Nimmo, E.R., Ekwall, K., Javerzat, J. and Cranston, G. (1995) *Genes Dev.*, **9**, 218–233.
- Lorentz, A., Osterman, K., Fleck, O. and Schmidt, H. (1994) *Gene*, **143**, 139–143.
- Ivanova, A.V., Bonaduce, M.J., Ivanov, S.V. and Klar, A.J.S. (1998) *Nature Genet.*, **19**, 192–195.
- Singh, P.B., Miller, J.R., Pearce, J., Kothary, R., Burton, R.D., Paro, R., James, T.C. and Gaunt, S.J. (1991) *Nucleic Acids Res.*, **19**, 789–794.
- Koonin, E., Zhou, S. and Lucchesi, J.C. (1995) *Nucleic Acids Res.*, **23**, 4229–4233.
- Aasland, R. and Stewart, A.F. (1995) *Nucleic Acids Res.*, **23**, 3168–3173.
- Paro, R. and Hogness, D.S. (1991) *Proc. Natl Acad. Sci. USA*, **88**, 263–267.
- Horsley, D., Hutchings, A., Butcher, G.W. and Singh, P.B. (1996) *Cytogenet. Cell Genet.*, **73**, 308–311.
- Zink, B. and Paro, R. (1989) *Nature*, **337**, 468–471.
- Murray, J.M., Carr, A.M., Lehmann, A.R. and Watts, F.Z. (1991) *Nucleic Acids Res.*, **19**, 3525–3531.
- Hoheisel, J.D., Maier, E., Mott, R., McCarthy, L., Grigoriev, A.V., Schalkwyk, L.C., Nizetic, D., Francis, F. and Lehrach, H. (1993) *Cell*, **73**, 109–120.
- Maudrell, K. (1993) *Gene*, **123**, 127–130.
- Chalfie, M., Tu, Y., Euskirchen, G., Ward, W.W. and Prasher, D.C. (1994) *Science*, **263**, 802–805.
- Niwa, O., Matsumoto, T., Chikashige, Y. and Yanagida, M. (1989) *EMBO J.*, **8**, 3045–3052.
- Kipling, D. and Kearsley, S.E. (1990) *Mol. Cell. Biol.*, **10**, 265–272.
- Hagan, I.M. and Hyams, J.S. (1988) *J. Cell Sci.*, **89**, 343–357.
- Woods, A., Sherwin, T., Sasse, R., MacRae, T.H., Baines, A.J. and Gull, K. (1989) *J. Cell Sci.*, **93**, 491–500.
- Jin, J.H., Yoo, E.J., Jang, Y.K., Kim, S.H., Kim, M.J., Shim, Y.S., Lee, J.S., Choi, I.S., Seong, R.H., Hong, S.H. and Park, S.D. (1998) *Mol. Gen. Genet.*, **257**, 319–329.
- Sawin, K.E. and Nurse, P. (1996) *Proc. Natl Acad. Sci. USA*, **94**, 15146–15151.
- Ekwall, K. and Ruusala, T. (1994) *Genetics*, **136**, 53–64.
- Boeke, J., LaCrute, F. and Fink, G.R. (1984) *Mol. Gen. Genet.*, **197**, 345–346.
- Toda, T., Umesono, K., Hirata, A. and Yanagida, M. (1983) *J. Mol. Biol.*, **168**, 251–270.
- Umesono, K., Toda, T., Hayashi, S. and Yanagida, M. (1983) *J. Mol. Biol.*, **168**, 271–284.
- Sandell, L.L. and Zakian, V.A. (1993) *Cell*, **75**, 729–739.
- Thon, G. and Klar, A.J.S. (1992) *Genetics*, **131**, 287–296.
- Egel, R., Willer, M. and Nielsen, O. (1989) *Curr. Genet.*, **15**, 407–410.